Published in final edited form as:
J Biomed Mater Res A. 2013 July ; 101(7): . doi:10.1002/jbm.a.34484.

Incorporation of fibronectin to enhance cytocompatibility in multilayer elastin-like protein scaffolds for tissue engineering

Swathi Ravi[1], **Jeffrey M. Caves**[2,3,4], **Adam W. Martinez**[1], **Carolyn A. Haller**[2,3,4], and **Elliot L. Chaikof**[1,2,3,4]

[1]Department of Biomedical Engineering, Georgia Institute of Technology/Emory University, Atlanta, Georgia 30332

[2]Department of Surgery, Emory University, Atlanta, Georgia 30322

[3]Department of Surgery, Beth Israel Deaconess Medical Center, Harvard Medical School, Boston, Massachusetts 02215

[4]Wyss Institute of Biologically Inspired Engineering, Harvard University, Boston, Massachusetts 02215

Abstract

Recombinant, elastin-like protein (ELP) polymers are of significant interest for the engineering of compliant, resilient soft tissues due to a wide range of tunable mechanical properties, biostability, and biocompatibility. Here, we enhance endothelial cell (EC) and mesenchymal stem cell compatibility with ELP constructs by addition of fibronectin (Fn) to the surface or bulk of ELP hydrogels. We find that cell adhesion, proliferation, and migration can be modulated by Fn addition. Adsorption of Fn to the hydrogel surface is more efficient than bulk blending. Surface immobilization of Fn by genipin crosslinking leads to stability without loss of bioactivity. Gels of varying mechanical modulus do not alter cell adhesion, proliferation, and migration in the range we investigate. However, more compliant gels promote an EC morphology suggesting tubulogenesis or network formation, whereas stiffer gels promote cobblestone morphology. Multilayer structures consisting of thin ELP sheets reinforced with collagen microfiber are fabricated and laminated through the culture of MSCs at layer interfaces. High cell viability in the resulting three-dimensional constructs suggests the applicability of Fn to the design of strong, resilient artificial blood vessels and other soft tissue replacements.

Keywords

protein polymer; elastin-mimetic; extracellular matrix; tissue engineering

INTRODUCTION

Performance of small-diameter vascular grafts is limited by thrombogenecity and neointimal hyperplasia, attributed in part to the different mechanical compliances of prosthetic and native tissue.[1,2] In the design of a bio-inspired artery replacement, recombinant elastin-like protein polymers (ELP) are under investigation because they are based on amino acid sequences from native, extracellular elastin, which is critical for the mechanical compliance

Correspondence to: E. L. Chaikof, M.D., Ph.D., 110 Francis St, Suite 9F, Boston, MA 02215; echaikof@bidmc.harvard.edu.

Additional Supporting Information may be found in the online version of this article.

of native arteries.[3] Triblock ELPs consist of hydrophilic, elastomeric midblock sequences flanked by self-associating, hydrophobic endblocks in an ABA block format.[4–6] These protein polymers are highly soluble under cool, aqueous conditions but self-assemble into elastomeric gels when warmed above an inverse transition temperature. This transition is driven by coacervation of the hydrophobic endblocks to form physical crosslinks, while the midblocks remain elastomeric and solvated. As an example, LysB10, a 209-kDa triblock ELP, has an inverse transition temperature of 13°C.[6] Our studies have shown that triblock ELPs are nonthrombogenic,[7] can be highly biostable,[8] permit controlled drug release,[9] and can be formed into multilayer composite tubes and sheets that mimic native soft tissue mechanics.[10,11]

Despite these features, the peptide sequences typically employed in ELP design do not support cell adhesion, proliferation, or migration. Here, we address this limitation by the incorporation of fibronectin (Fn) into ELP materials. In the context of related strategies that covalently link peptides to ELPs[12] or add cell-adhesive domains directly to the ELP backbone,[13] the blending and adsorption methods described here may present a more efficient and versatile route to cytocompatibility.

Fn is an adhesive glycoprotein secreted by cells to form a fibrillar matrix and regulates functions such as cell cycle progression, migration, differentiation, and assembly of other extracellular matrix (ECM) components.[14–16] Unlike short peptide adhesive sequences, Fn contains multiple sites for functional engagement. The monomeric Fn molecule is 220 kDa, but the functional unit exists as a disulfide-cross-linked heterodimer. The arginine-glycine-aspartic acid (RGD) and synergy cell-binding sequences interact directly with integrins on the cell surface, whereas binding sites for heparin, collagen, and fibrin molecules modulate the microenvironment around the cells.

Due to the role of the endothelium as a bioactive, thromboresistant barrier, some vascular prosthetics have been designed to retain a quiescent EC layer, with clear benefit.[17] Early tissue-engineered blood vessel (TEBV) prototypes further mimicked the vascular media by including smooth muscle cells (SMC).[18] However, due to the challenges of autologous SMC sourcing, alternative cells have been suggested, including autologous bone marrow mononuclear cells[19] and various progenitor cells.[20–22] Moreover, cells seeded within the TEBV wall have recently been regarded by some as transient components to generate ECM scaffolding exclusively *in vitro*[23,24] or to secrete cytokines for a few days following implant.[25] In this study, we investigate compatibility with ECs as well as bone-marrow mesenchymal stem cells (MSC) as a potential TEBV-wall cell. In addition to offering convenience as a readily expandable autologous source, and the immunomodulatory effects of allogenic transplants,[26,27] MSCs may be antithrombogenic[28] and capable of differentiation into endothelial-like[29] or smooth muscle cell-like[30] cells.

MATERIALS AND METHODS

Reagents and cells

Porcine mesenchymal stem cells (pMSCs) were a kind gift from Dr. Steven Stice (University of Georgia). The biosynthetic strategy for the expression and purification of the recombinant ELP triblock polymer, LysB10, has been described previously.[6] Briefly, the LysB10 sequence is encoded in a single contiguous reading frame within the expression plasmid pET24-a, transformed to *Escherichia coli* BL21(DE3). Scale expression of 1 L was performed at 37°C in Circle Grow medium supplemented with kanamycin (50 μg/mL) in Fernbach shake flasks for 24 h. Harvested expression pellets were lysed through three freeze/thaw cycles and sonication. A series of warm/cold centrifugations were utilized to

purify ELP from the total expression lysate; after 6 to 10 cycles, material was dialyzed and lyophilized.

Determination of percent extractable protein

Circular films (d = 1 cm) were cast from 10 wt% LysB10 in water at 4°C. After drying, films were crosslinked in 6 mg/mL genipin (Wako) solutions for 24 h and rinsed in ddH_20 for 12 h, with buffer changes to remove residual crosslinker. The weight of dried films was recorded prior to incubating them in water at 4°C (below the inverse transition temperature). After a 7-d incubation, films were dried and weighed to determine material loss. The mass retention (MR) was calculated with the equation $MR = [W_f/W_i] \times 100\%$, where W_f and W_i are the final and initial dehydrated weights, respectively.

Mechanical compression

Solutions of LysB10 (10 or 6 wt%, in 4°C ddH_2O) were loaded into 1 mL syringes (inner diameter = 4.67 mm) and gelled by warming at 37°C. The syringe tip was cut off, and the protein polymer gel extruded into PBS and sectioned into 2-mm-thick discs. Gel discs were placed in 1 mg/mL Fn (Sigma Aldrich) solution for 4 h and then crosslinked in genipin and rinsed. Gels were also crosslinked in genipin without incubation in Fn. Compression measurements were acquired on a Bose ELF system with a 10 lb load cell and a hydration chamber containing PBS at 37°C; gels were fully hydrated prior to testing to prevent any confounding effects from swelling. Samples were preconditioned by compression from 1% to 20% strain for 10 cycles. Compression stress–strain testing was performed at 0.025 mm/s with compressive force monitored over time. Cotangent moduli were calculated from the compression stress–strain plots at 10% intervals from 20% to 40%. The cotangent was calculated by performing a linear regression on the points at a given percent strain ± 1% strain. Stress relaxation was measured by compressing the samples to a strain of 50% using a crosshead speed of 0.025 mm/s, and then allowing the crosshead to rest for 15 min or longer until force decay was minimal (0.001 MPa/min).

Fn-blended and Fn-adsorbed protein polymer hydrogels

Fn-LysB10-blended solutions were formulated by adding lyophilized LysB10 at 10 or 6 wt % to appropriate dilutions of Fn in PBS at 4°C and mixing for 16 h. In contrast to blended specimens, the protein polymer solutions for adsorbed specimens were prepared without Fn. The well bottoms of polystyrene 96-well plates, pre-cooled at 4°C, were uniformly coated with 40 μL of protein polymer solution. Hydrogel formation was achieved by transfer at 37°C for 1 h. Fn-adsorbed specimens were then incubated in 1 mg/mL Fn solutions for 6 h at room temperature. Genipin crosslinking and rinsing were performed on both blended and adsorbed specimens as detailed above.

The extent of Fn immobilization on hydrogel surfaces was determined with a solid-phase enzyme immunoassay (EIA kit, Takara Bio). Fn-adsorbed hydrogels were created in EIA wells as described above, with the concentration of the Fn solution varied from 0 to 1 mg/mL. Fn density was assessed according to the manufacturer's protocol, with absorbance at 450 nm compared to standard curves.

Adhesion and proliferation of endothelial and MSC

Human umbilical vein endothelial cells (HUVECs, Clonetics) were cultured in endothelial growth medium-2 (EGM-2, 2% serum, Clonetics). Porcine bone marrow-MSCs were cultured in αMEM supplemented with 10% FBS, 50 U/mL penicillin, 50 μg/mL streptomycin, and 2 mM L-glutamine. HUVECs and MSCs between passages 3 and 9 were harvested with cell dissociation solution (Sigma) and re-suspended at 200,000 cells/mL,

with HUVECs in αMEM supplemented with 0.5% bovine serum albumin (BSA) and MSCs in low-serum medium (1% FBS). Cells (100 μL) were added to hydrogel-coated wells, incubated at 37°C for 2 h, and washed three times with PBS. Cell adhesion was quantified with the CyQuant cell proliferation assay kit (Molecular Probes) according to the manufacturer's protocol. Micro-plate spectrofluorometer measurements were normalized to results from Fn-coated polystyrene wells, a positive control.

The stability of the incorporated Fn was assessed after incubating noncrosslinked and genipin-crosslinked hydrogels in PBS for 7 d, with daily PBS changes. Following the incubation, a HUVEC adhesion assay was performed as described above.

Proliferation rates were evaluated by adding HUVECs and MSCs on various hydrogel surfaces (5000 cells/well). After 2 h, unbound cells were removed with media washes, and substrate-bound cells were maintained in culture for 48 h. Cell adhesion was quantified with the CyQuant kit at 2 and 48 h.

Endothelial cell migration on protein polymer hydrogels

HUVEC migration on LysB10 and Fn-coated wells was defined using the Oris cell migration assay FLEX kit (Platypus Technologies). A cell-seeding stopper (d = 2 mm) was positioned on the hydrogel surface. Cells were harvested, treated with mitomycin C (10 μg/mL, Sigma), and re-suspended at 400,000 cells/mL in serum-free basal media. One hundred microliters of cell suspension was seeded on the outer annular region of the protein gel surfaces (30 mm^2) and allowed to adhere for 6 h at 37°C, at which point the stoppers were removed to permit migration into the detection zone. Following seeding, wells were rinsed with media and incubated for 36 h. Wells were washed with PBS, stained with calcein AM, and analyzed with a fluorescent plate reader. The Oris detection mask restricted signal collection to cells within the migration detection zone. A background signal was collected from wells with stoppers left in place until signal collection and subtracted from the measurements. Data were normalized to migration data collected from Fn-coated wells.

Immunofluorescence characterization of cell morphology and HUVEC activation

Morphology was observed by fluorescently labeling of actin and vinculin while HUVEC activation state was visualized with ICAM-1 and E-selectin. Fn control surfaces were formulated by adsorbing 50 μg/mL solutions overnight at 4°C. HUVECs were seeded in polystyrene 8-well chamber slides coated with the experimental surface and cultured for 2 h (F-actin staining) or 4 h (ICAM-1 and E-selectin staining) in serum-free medium. Similarly prepared pMSCs were cultured in low-serum (1% FBS) media. HUVECs were activated with 100 ng/mL TNFα added for 4 h to cells cultured on Fn control surfaces. Specimens were prepared by fixation in paraformaldehyde, permeabilized with PBS containing 0.5% Triton X-100, rinsed with 100 mM glycine, and incubated with block buffer (PBS+/+, 0.2% Triton X-100, and 6% goat serum). For F-actin staining, cells were incubated with Alexa Fluor 568-conjugated phalloidin. HUVEC activation was probed with 10 μg/mL solutions of E-selectin and ICAM-1 monoclonal antibodies. Incubation was followed by secondary incubation with biotinylated goat anti-mouse IgG and tertiary incubation with streptavidin-AlexaFluor 488. Nuclei were counterstained with DAPI, and specimens were evaluated with confocal microscopy.

Generation of MSC-seeded, collagen fiber-reinforced laminates

ELP sheets (thickness = 50 μm) reinforced with collagen microfibers[31] at prescribed angles and densities were fabricated as previously described.[10] Sections of the sheet (1 × 1 cm) were incubated in 1 mg/mL Fn, with both sides treated for 6 h. Genipin crosslinking and

rinsing were performed as described above, following which sheets were subject to an additional cycle of Fn adsorption in order to maximize cell adhesion.

MSCs were seeded onto Fn-treated protein polymer sheets via a two-stage seeding following a standard technique. Seeded sheets were transferred into fresh wells and incubated in media for 72 h, or until a confluent monolayer was observed, with a change of media after 2 days. Sheets with confluent MSC layers were stacked into two and three sheet laminates and sandwiched between sterile nylon meshes with 70 μm pores; nylon meshes were utilized as the outermost top and bottom layers to facilitate compression and lamination of sheets. Constructs were cultured for 7 d, with media changed every 2 d, to facilitate interlamellar bonding.

MSC viability, morphology, and inflammatory potential on protein polymer sheets

Cell-seeded single sheets and laminated constructs were removed from culture and incubated in 2 μM calcein AM solution for 1 h at room temperature and imaged with laser scanning confocal microscopy. Cell-seeded laminates that were maintained in culture for 1 week were fixed in 4% paraformaldehyde overnight prior to flash-freezing in OCT medium and cryosectioning. Sections were incubated in hemotoxylin and eosin and alcian blue staining with nuclear fast red counterstain to visualize glycosaminoglycan deposition.

Messenger RNA levels of interleukin-1β (IL-1β) and cyclooxygenase-2 (COX-2) were analyzed with reverse transcriptase polymerase chain reaction (RT-PCR) using glyceral-dehyde-3-phosphate-dehydrogenase (GAPDH) as the internal control. All primers were obtained from Applied Biosystems. MSC-seeded tri-lamellar constructs were cultured for 96 h prior to RNA isolation; results were compared to MSCs maintained for 96 h on tissue-culture-treated polystyrene (TCPS) with and without 10 μg/mL lipopolysaccharide (LPS). All PCR reactions were performed in triplicate with 50 ng of cDNA using the Taqman PCR system (Applied Biosystems). Data were normalized to TCPS-MSC cultures without LPS activation.

RESULTS

Bulk and surface-immobilized Fn promote endothelial cell compatibility

A 2 h HUVEC adhesion assay demonstrated that both modes of Fn incorporation affect EC adhesion, although improved results were seen with surface adsorption. Blending Fn into hydrogel bulk at ratios of 0.05 to 0.75 mol% demonstrated a trend toward enhanced levels of adhesion (Fig. 1). The greatest effect was observed when the Fn coatings were adsorbed to the hydrogel surface (“Fn on LysB10,” Fig. 1). Incorporating Fn in this way produced HUVEC adhesion levels in the range of 80% of the positive control surface, consisting of Fn adsorbed to non-tissue culture-treated polystyrene. In addition, biostability studies revealed that genipin crosslinking after Fn adsorption leads to a sustained bioactive effect following a 7 d incubation in PBS [Fig. 2(a)]. However, in the absence of crosslinking, the cell-adhesive effect of adsorbed Fn did not persist after the incubation period. Given these results, the surface-adsorbed, genipin-crosslinked Fn-LysB10 was subject to further analysis. We characterized Fn density on both 6 and 10 wt% hydrogels. Enzyme immunoassay indicated that passive adsorption followed by genipin crosslinking produced immobilized Fn coatings at ligand densities in the range of 5–150 fmol/cm^2. Density depended both on the protein polymer content of the hydrogel (6 or 10 wt%) and on the concentration of the Fn solution (Fig. 2b).

Measurements of EC proliferation and migration were consistent with the adhesion measurements. Proliferation was not observed for 6 or 10 wt% LysB10 without Fn [Fig. 3(a,b)]. The greatest proliferation occurred with surface-adsorbed Fn that was immobilized

by genipin crosslinking, with fluorescent signal approximately tripling after 48 h [Fig. 3(a,b)]. In contrast, blended Fn hydrogels led to a sig-nificantly lower signal that approximately doubled over the proliferation period. Results from the HUVEC migration assay paralleled these observations, with surface-immobilized Fn yielding the greatest migratory behavior for both 6 and 10 wt% hydrogels [Fig. 3(c,d)]. In the case of 10 wt% hydrogels, blending Fn into the bulk of the gel failed to elicit any measurable migratory response. Mechanical compression testing confirmed that, while genipin crosslinking elevates gel stiffness, surface-adsorbed Fn does not alter hydrogel mechanics [Fig. 4(a–d), Supporting Information Table SI]. Studies of percent mass retention indicated that, while uncrosslinked LysB10 films dissolved in cold water, genipin crosslinked films retained ~ 93.5 ± 1.4% of their mass, consistent with a high degree of chemical crosslinking.

The morphology of ECs on protein polymer-Fn surfaces was evaluated through immunostaining of F-actin stress fibers and vinculin. Compared to hydrogels lacking surface-immobilized Fn [Fig. 5(c,d,g,h)], HUVECs on the experimental Fn surfaces developed extensive actin stress fiber networks and vinculin clusters [Fig. 5(e,f,i,j)]. A monolayer of HUVECs with characteristic cobblestone morphology was observed on all crosslinked Fn-LysB10 hydrogels and 10 wt% noncrosslinked Fn-LysB10. However, alternate EC morphology was observed on the lowest-modulus surface investigated, noncrosslinked 6 wt% Fn-LysB10 (Fig. 6). In these samples, vinculin and actin staining revealed the formation of cordlike structures and networks of elongated HUVECs after 2 h culture, indicating tubule formation. In addition to these morphological observations, immunofluorescence was used to assess HUVECs activation. Expression of ICAM-1 and E-selectin on crosslinked LysB10-Fn surfaces was consistent with quiescent controls (Fig. 7).

Fn also promotes MSC compatibility on protein polymers

Similar quantification of adhesion and proliferation of MSCs seeded on protein polymer-Fn surfaces indicated cytocompatibility. Concentrations of either 0.25 mg/mL or 1.00 mg/ mL were adsorbed to 10 wt% surfaces, which were previously observed to generate ligand surface densities of ~ 82 and 153 fmol/cm^2 [Fig. 2(b)]. Adhesion rates ranged from ~ 50 to 80% of positive controls and increased with Fn surface density, while few MSCs adhered to protein polymer surfaces lacking Fn [Fig. 8(a)]. Proliferation rates were also significantly enhanced by the presence and density of Fn and increased slightly with protein polymer content from 6 to 10 wt% [Fig. 8(b)].

Sheet-based protein polymer MSC composites

We explored the feasibility of constructing stable, cellularized laminates from protein polymer sheets and MSCs with the aid of adsorbed Fn. Sheets of protein polymer reinforced with collagen microfiber[10] were subjected to an Fn-adsorbed protocol and seeded with MSCs. Stacks of two or three sheets with confluent MSC layers were sandwiched between nylon meshes to maintain contact between the sheets. When constructs were handled after 7 d in culture, the development of limited mechanical bonding at the sheet interfaces was observed. Calcein AM staining indicated high viability of each cell layer following the week-long culture [Fig. 9(a,b,e,f)]. Moreover, histological preparations of single sheets and stacked constructs demonstrated that MSCs persist in organized layers within the composite structure [Fig. 9(c,d,g,h)]. Intermittent deposition of glycosaminoglycans was observed at the sheet interfaces. RT-PCR was used to investigate expression of IL-1β and COX-2. After 96 h culture, expression of these inflammatory upregulators was comparable to negative controls, suggesting no tendency towards a pro-inflammatory phenotype (Fig. 10).

DISCUSSION

ELP polymers have shown promising biocompatibility,[8] blood-contacting properties,[7] and mechanical properties[11] for use in tissue-engineered blood vessels but have required modification to enhance cytocompatibility.[12,13] In this study, Fn was selected to support cellular adhesion, as a multifunctional ligand that binds directly to cells, as well as heparin, collagen, and fibrin molecules, thereby modulating the ECM microenvironment.[14–16] Fn has been investigated by several groups to enhance endothelialization of vascular graft surfaces both *in vitro* and *in vivo*.[32] For example, covalently bound Fn on ePTFE graft lumens was shown to accelerate transmural tissue ingrowth and neointima formation in a canine model and was associated with significantly lower thrombus area.[33]

As anticipated, Fn enhanced cell behaviors both as an adsorbed surface coating and when blended into hydrogel bulk. Greater proliferation and migration were found with the adsorption method compared to blending, possibly because this method concentrated Fn ligands at the surface of the material. On the adsorbed surfaces, hydrogels with a higher level of protein polymer (10 vs. 6 wt%) tended to have a higher density of adsorbed ligand. This difference is most likely due to an increased density of LysB10 molecules at the 10 wt % gel surface, which in turn would facilitate greater Fn adsorption.

Our exploration of the stability of incorporated Fn revealed that crosslinking was required to retain surface bioactivity after prolonged incubation in PBS. Intermolecular crosslinking with genipin is thought to occur via the primary amine groups and the C3 carbon of genipin, with subsequent dimerization produced by radical reactions.[34,35] Notably, this finding suggests that genipin crosslinking immobilizes adsorbed Fn without substantially interfering with bioadhesive sites. Crosslinking may also provide more desirable mechanical properties for a vascular graft construct, specifically reducing ELP creep strain.[6,11]

The mechanical properties of the ECM can play a vital role in determining cell fate. Stiffness influences a range of cell processes, including adhesion, proliferation, migration, tubulogenesis, focal adhesion formation, and differentiation potential.[36–38] In general, cell adhesion and growth increase as substrate stiffness increases, until a threshold is reached, beyond which cell response does not vary. For example, a greater fibroblast proliferation rate and a 50% decrease in apoptosis have been reported on 14-kPa gels compared to 4.7-kPa gels.[39] Moreover, stiffer substrates have been reported to promote cell spreading, with the greatest degree of spreading noted on 10-kPa gels and no further increase in the spread area beyond that value.[40,41] Increased recruitment of vinculin to adhesion sites has been noted on stiffer substrates as well.[42]

Here, we varied gel stiffness by employing protein polymer concentrations of 6 or 10wt%, with a constant Fn surface density. We accounted for differences in the Fn adsorption profile of these gels by adsorbing 1 or 0.25 mg/mL Fn to the 6 or 10 wt% gel, respectively. These parameters led to a ligand density of 82 fmol/cm^2 on gels of different stiffness (42 or 106 kPa, at low strains). In this range, we did not find that gel modulus affected EC proliferation and migration. However, altering Fn density from 82 to 153 fmol/cm^2 on 10 wt% gels, by adsorbing 1 mg/mL Fn instead of 0.25 mg/mL, stimulated higher endothelial proliferation and migration rates. As a comparison, others have reported that an Fn density of 140 fmol/cm^2 is required in inducing maximal cell adhesion.[43]

The formation of blood vessels from ECs, or tubulogenesis, is a multistep process in which alignment of ECs and generation of a patent lumen is induced by biochemical and mechanical factors.[44,45] Numerous groups have demonstrated that the formation of cordlike structures and networks of elongated cells are governed by a combination of ligand density

and substrate modulus. For example, Califano and colleagues observed cord-like formation of ECs on 1-kPa polyacrylamide substrates derivatized with type I collagen, while cells on 10-kPa gels formed evenly distributed monolayers.[46] However, when collagen density was decreased 100-fold, network formation was seen on 10-kPa gels as well. Similarly, Deroanne and colleagues have reported the formation of cordlike structures on 17-kPa matrigel while cells on 75-kPa gels formed a monolayer.[47] By staining for actin and vinculin, we observed that ECs assumed a spread morphology on all Fn-LysB10 surfaces, with varying cell patterning correlating to gel stiffness. In this case, modulation of the compressive modulus from 42 kPa to ~ 9 kPa (crosslinked vs. uncrosslinked 6 wt% hydrogel) triggered formation of elongated cells and the assembly of tube-like structures. This confirmed previous reports that a decrease in mechanical resistance is sufficient to switch EC patterning from a monolayer to differentiated tube-like structures. Note that we performed all studies at a constant genipin concentration (6 mg/mL); future studies may examine the ability of crosslinking to control ELP stiffness as a function of genipin concentration. Collectively, these results illustrate the potential to tune the biological response of ECs from a tube-like morphology, which may be desirable to promote vasculogenesis, to a cobblestone morphology, which may be advantageous in promoting the formation of a vascular lumen.

The interplay between substrate stiffness and ligand presentation also directs MSC behavior. MSCs are multipotent adult stem cells that can differentiate into a number of cell types, including osteoblasts, chondrocytes, vascular ECs, and cardiomyocytes.[48–50] Similarities of porcine MSCs with their human counterparts make them ideal candidates for *in vitro* studies and preclinical investigations and have contributed to enhanced wound healing, angiogenesis, myocardial viability, and bone formation.[51] Although survival and differentiation remain the primary objective of MSC biomaterial incorporation, a transitory population may also support an improved healing response through the paracrine action of the MSC secretome. The attachment of MSCs on polyacrylamide gels is dependent not only on gel stiffness, but also on the type of ECM molecule presented on the surface of the gel.[52] In general, stiffer gels supported higher cell adhesion and proliferation than the softer ones (in the range of 0.7–80 kPa), with similar proliferation rates on gels of 25 kPa and higher. Moreover, at 25 kPa and higher, Fn-coated gels supported the highest number of adherent MSCs, with collagen I, laminin, and collagen IV coatings supporting adhesion to a lesser degree. Our studies of MSC behavior on Fn-LysB10 gels yielded similar results to those of ECs, with maximal adhesive and proliferative responses achieved with crosslinked 10 wt% gels with 1 mg/mL adsorbed Fn.

Three-dimensional reconstruction of functional tissues with cell sheet technology is under intensive investigation. For example, the temperature-responsive polymer poly(*N*-isopropylacrylamide) (PIPAAm) enables culturing of cells and facilitates the harvest of confluent cells as intact sheets.[53] Promising applications of this technology have been the layering of MSC sheets for the development of tissue-engineered cardiac patches as well as the creation of organ-like tubular structures.[54,55] Other investigators have utilized prolonged culture periods and the addition of media supplements to stimulate increased matrix deposition of cultured cells to generate mechanically robust cell sheets that can be rolled into vascular conduits.[56] Previously, we fabricated multilayer sheets and tubes from collagen fibers and elastin-mimetic recombinant proteins and found that this architecture allows for control of scaffold mechanics, including compliance, resilience, strength, and anisotropy.[10,11] Here, we confirmed MSC viability on similar sheet-based structures and evaluated the inflammatory potential of these constructs. Although positive controls indicated high expression of both IL-1β and COX-2, MSCs maintained an anti-inflammatory phenotype in experimental multilayer protein-sheet constructs.

In conclusion, EC and MSC compatibility with ELP hydrogels and multilayer constructs was affected through the addition of Fn. We quantified cell adhesion, proliferation, and migration at levels approaching positive control surfaces. Adsorption of Fn to the hydrogel surface was more efficient than bulk blending, and genipin crosslinking durably immobilized Fn to the surface without obstructing cell-adhesive sites. In the range explored, gel mechanics did not alter cell adhesion, proliferation, and migration, although softer surfaces promoted EC network formation. ECs were quiescent, and MSCs did not express pro-inflammatory markers on the experimental surfaces. The fabrication of multilayer, fiber-reinforced constructs with high cell viability suggests the applicability of Fn to the design of strong, resilient artificial blood vessels as well as replacements for other soft tissues with multilayered architecture.

Supplementary Material

Refer to Web version on PubMed Central for supplementary material.

References

1. Abbott WM, Megerman J, Hasson JE, L'Italien G, Warnock DF. Effect of compliance mismatch on vascular graft patency. J Vasc Surg. 1987; 5:376–382. [PubMed: 3102762]
2. Conte MS. The ideal small arterial substitute: A search for the Holy Grail? FASEB J. 1998; 12:43–45. [PubMed: 9438409]
3. Patel A, Fine B, Sandig M, Mequanint K. Elastin biosynthesis: The missing link in tissue-engineered blood vessels. Cardiovasc Res. 2006; 71:40–49. [PubMed: 16566911]
4. Wright ER, Conticello VP. Self-assembly of block copolymers derived from elastin-mimetic polypeptide sequences. Adv Drug Deliv Rev. 2002; 54:1057–1073. [PubMed: 12384307]
5. Nagapudi K, Brinkman WT, Thomas BS, Park JO, Srinivasarao M, Wright E, Conticello VP, Chaikof EL. Viscoelastic and mechanical behavior of recombinant protein elastomers. Biomaterials. 2005; 26:4695–4706. [PubMed: 15763249]
6. Sallach RE, Cui W, Wen J, Martinez A, Conticello VP, Chaikof EL. Elastin-mimetic protein polymers capable of physical and chemical crosslinking. Biomaterials. 2009; 30:409–422. [PubMed: 18954902]
7. Jordan SW, Haller CA, Sallach RE, Apkarian RP, Hanson SR, Chaikof EL. The effect of a recombinant elastin-mimetic coating of an ePTFE prosthesis on acute thrombogenicity in a baboon arteriovenous shunt. Biomaterials. 2007; 28:1191–1197. [PubMed: 17087991]
8. Sallach RE, Cui W, Balderrama F, Martinez AW, Wen J, Haller CA, Taylor JV, Wright ER, Long RC Jr, Chaikof EL. Long-term biostability of self-assembling protein polymers in the absence of covalent crosslinking. Biomaterials. 2009; 31:779–791. [PubMed: 19854505]
9. Nagapudi K, Brinkman W, Leisen J, Thomas B, Wright E, Haller C, Wu X, Apkarian R, Conticello V, Chaikof E. Protein-based thermoplastic elastomers. Macromolecules. 2005; 38:345–354.
10. Caves JM, Cui W, Wen J, Kumar VA, Haller CA, Chaikof EL. Elastin-like protein matrix reinforced with collagen microfibers for soft tissue repair. Biomaterials. 2011; 32:5371–5379. [PubMed: 21550111]
11. Caves JM, Kumar VA, Martinez AW, Kim J, Ripberger CM, Haller CA, Chaikof EL. The use of microfiber composites of elastin-like protein matrix reinforced with synthetic collagen in the design of vascular grafts. Biomaterials. 2010; 31:7175–7182. [PubMed: 20584549]
12. Ravi S, Krishnamurthy VR, Caves JM, Haller CA, Chaikof EL. Maleimide-thiol coupling of a bioactive peptide to an elastin-like protein polymer. Acta Biomater. 2011; 8:627–635. [PubMed: 22061108]
13. Ravi S, Haller CA, Sallach RE, Chaikof EL. Cell behavior on a CCN1 functionalized elastin-mimetic protein polymer. Biomaterials. 2012; 33:2431–2438. [PubMed: 22212194]
14. Sakai T, Larsen M, Yamada KM. Fibronectin requirement in branching morphogenesis. Nature. 2003; 423:876–881. [PubMed: 12815434]

15. Sechler JL, Schwarzbauer JE. Control of cell cycle progression by fibronectin matrix architecture. J Biol Chem. 1998; 273:25533–25536. [PubMed: 9748212]
16. Yamada KM. Cell surface interactions with extracellular materials. Annu Rev Biochem. 1983; 52:761–799. [PubMed: 6351729]
17. Zilla P, Deutsch M, Meinhart J. Endothelial cell transplantation. Semin Vasc Surg. 1999; 12:52–63. [PubMed: 10100386]
18. Weinberg CB, Bell E. A blood vessel model constructed from collagen and cultured vascular cells. Science. 1986; 231:397–400. [PubMed: 2934816]

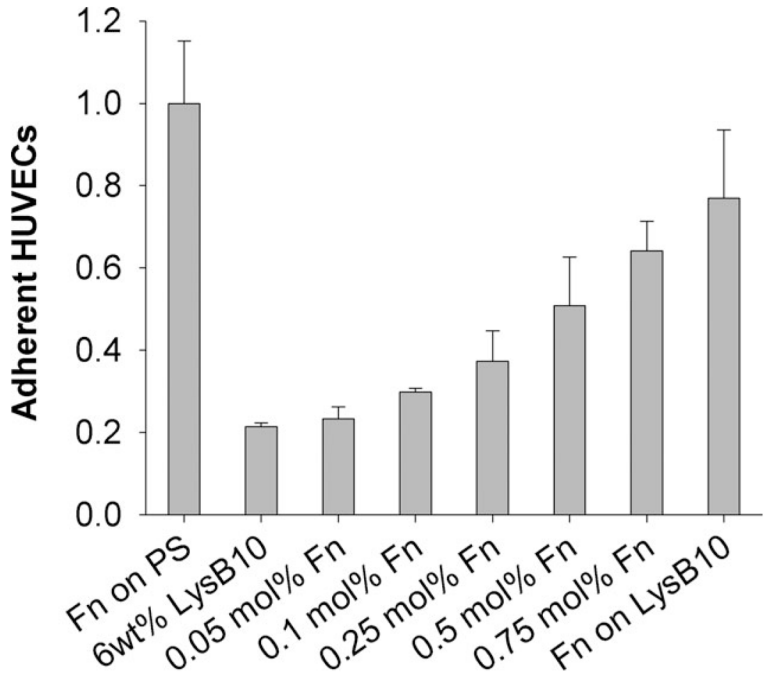

FIGURE 1.

HUVEC adhesion. Quantification of HUVEC adhesion after 2 h, in 0.05–0.75 mol% blends of Fn and 6 wt% LysB10, as well as surface-adsorbed Fn (from a 1 mg/mL solution, titled "Fn on LysB10"). Data normalized to a positive control of 50 μg/mL Fn adsorbed to polystyrene overnight.

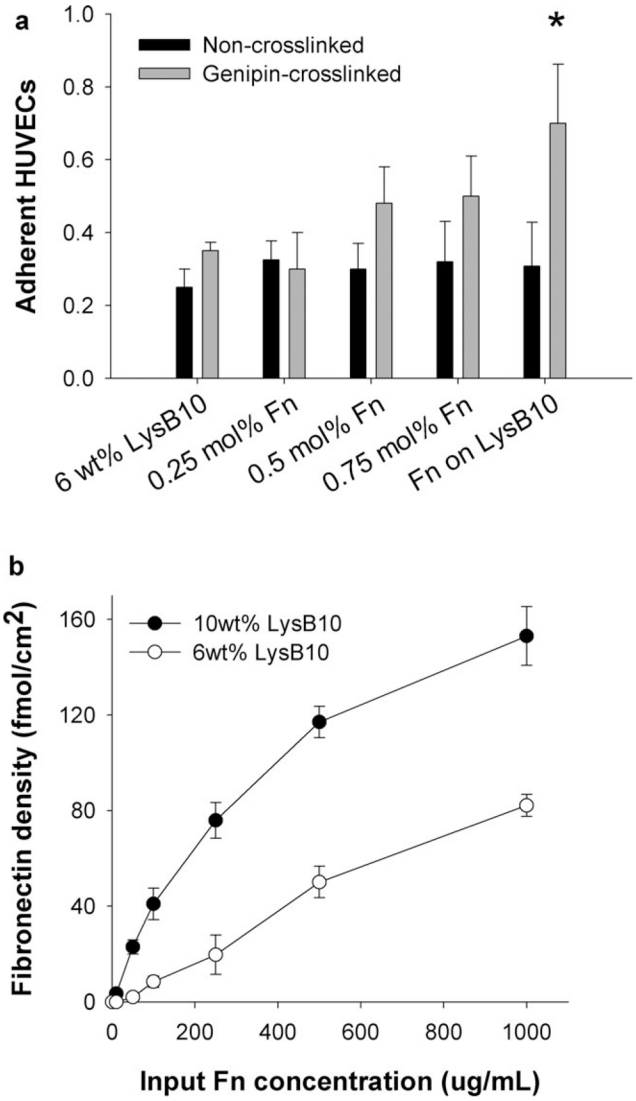

FIGURE 2.

Characterization of surface-adsorbed Fn. (a) Stability of adsorbed Fn, determined by measuring adhesion levels after 1 week incubation in PBS prior to performing the 2-h adhesion assay. * $p < 0.05$ compared to noncrosslinked counterparts. (b) Fn ligand density after crosslinking on 10 or 6 wt% LysB10 hydrogel surfaces as a function of input Fn concentration. Data represent one of three similar experiments, with each condition run in quadruplicate.

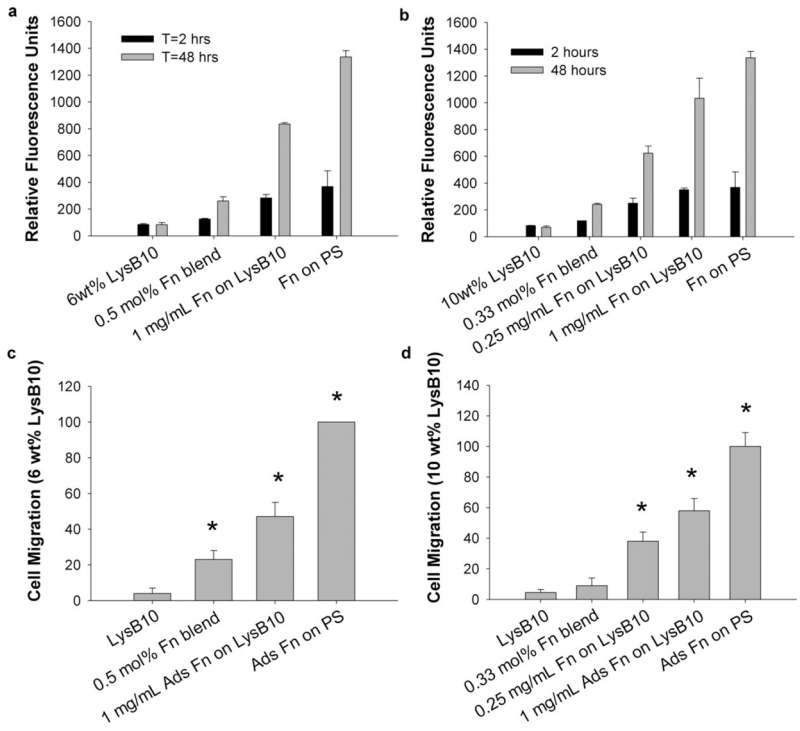

FIGURE 3.

HUVEC proliferation and migration on crosslinked hydrogels. (a,b) HUVEC proliferation on crosslinked Fn-LysB10 gels after seeding 5000 cells/well for 48-h periods on 6 and 10 wt % gel formulations, respectively. Nonadherent cells were removed after 2 h, and cell number measured after 2 or 48 h. (c,d) HUVEC migration on crosslinked Fn-LysB10 gels after seeding 40,000 cells onto an outer annulus area and monitoring for motility into an inner radial zone on (c) 6 wt% crosslinked hydrogels and (d) 10 wt% crosslinked gels over a 36-h period. Quantification was achieved with fluorescent measurement of the number of migrated cells into the detectable inner zone, which was normalized against the number of migrated cells on Fn-coated polystyrene. * $p < 0.05$ compared to unmodified LysB10.

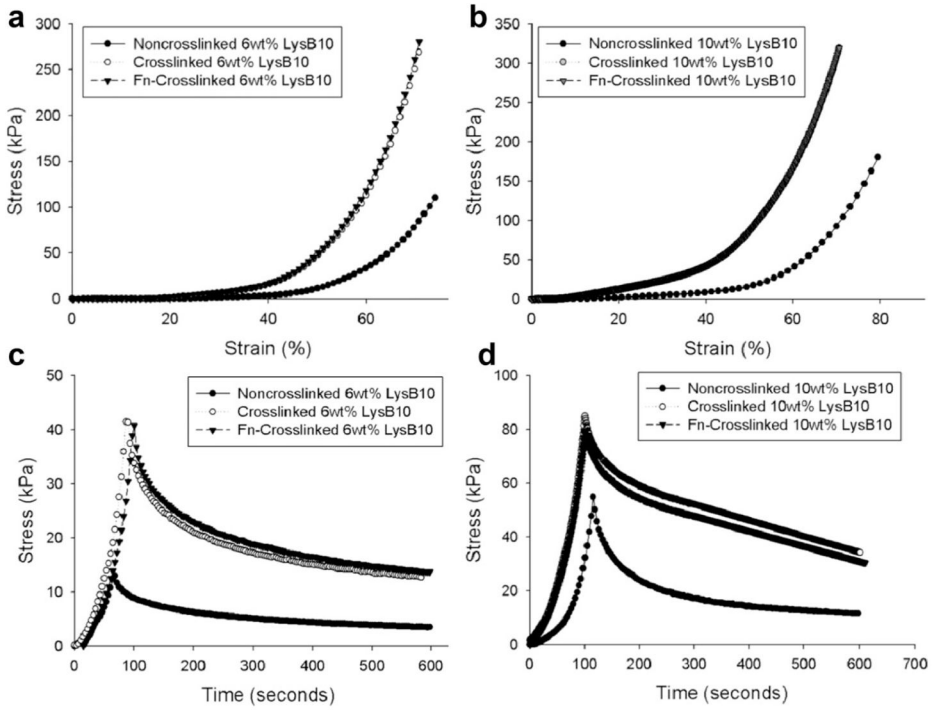

FIGURE 4.

Mechanical compression. (a,b) Representative compression tests of LysB10 hydrogels. Treatment groups include noncrosslinked LysB10, genipin-crosslinked LysB10, and adsorbed Fn that has been genipin-crosslinked on LysB10. (c,d) Compressive stress relaxation of similar experimental groups at 50% strain.

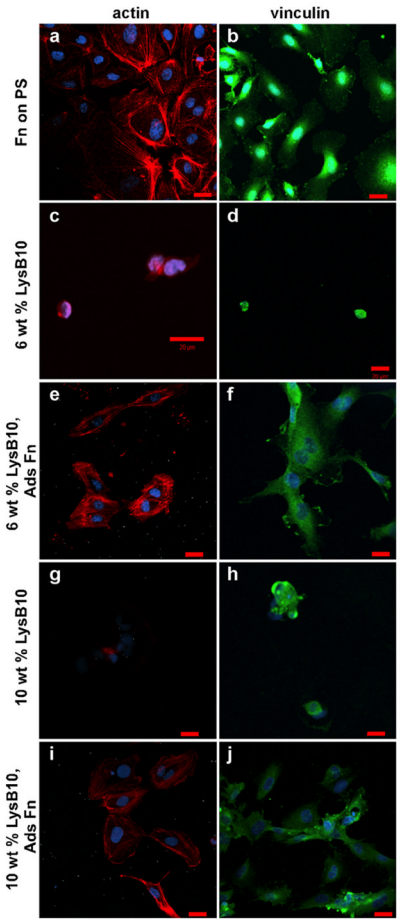

FIGURE 5.

HUVECs cultured on crosslinked ELP substrates. As indicated, 1 mg/mL Fn was adsorbed onto LysB10 gels and crosslinked with genipin. Fluorescently labeled actin is shown in red (a,c,e,g,i), whereas vinculin is displayed in green (b,d,f,h,j). Scale 20 μm. [Color figure can be viewed in the online issue, which is available at wileyonlinelibrary.com.]

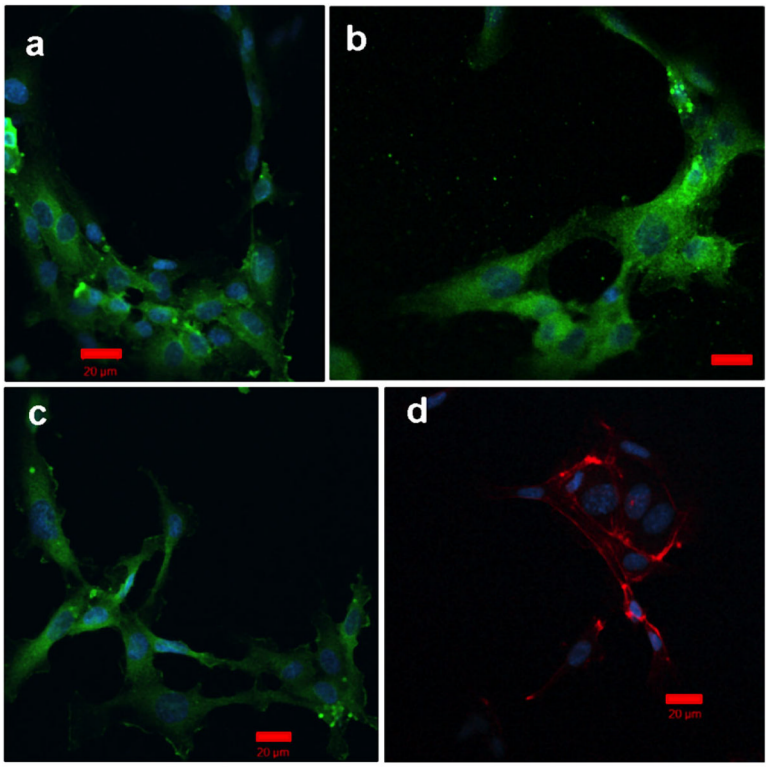

FIGURE 6.
HUVECs cultured on uncrosslinked Fn-LysB10 gels. A total 1 mg/mL Fn was adsorbed onto LysB10 gels for 6 h prior to cell seeding. Fluorescently labeled actin is displayed in red (d), whereas vinculin is displayed in green (a,b,c). Scale 20 μm. [Color figure can be viewed in the online issue, which is available at wileyonlinelibrary.com.]

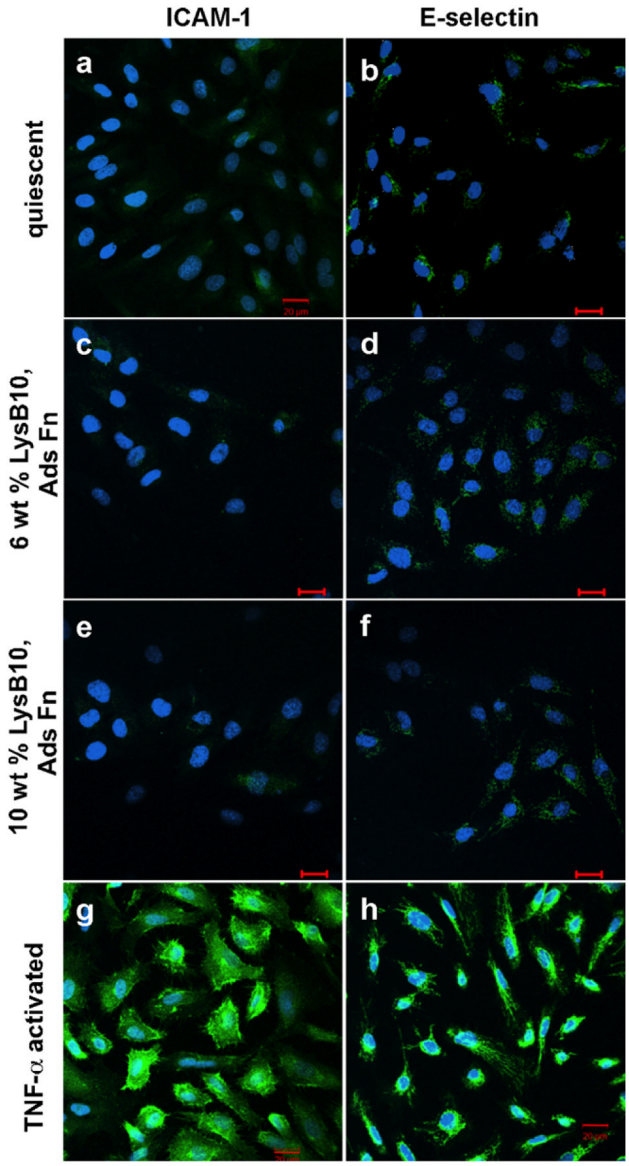

FIGURE 7.

Quiescence of HUVECs cultured on crosslinked ELP substrates. Cells that were cultured on Fn-coated slides without TNF-α stimulation (a,b) maintained a quiescent phenotype. Activation was achieved with the addition of TNF-α to the culture medium (g,h). HUVEC activation or quiescence was compared to that on crosslinked Fn-modified LysB10 films (c,d,e,f). Markers of HUVEC activation were ICAM1-1 (a,c,e,g) and E-selectin (b,d,f,h). Scale 20 μm. [Color figure can be viewed in the online issue, which is available at wileyonlinelibrary.com.]

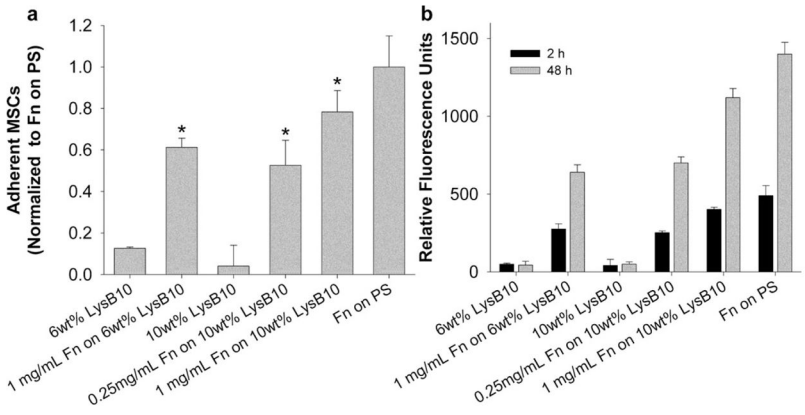

FIGURE 8.

MSC adhesion and proliferation on crosslinked Fn-LysB10. (a) A 2-h adhesion assay on crosslinked LysB10 gels with surface-immobilized Fn. Data normalized to a positive control, 50 μg/mL Fn adsorbed to polystyrene overnight. * $p < 0.05$ compared to LysB10 counterparts without Fn. (b) MSC proliferation over a 48-h period on crosslinked LysB10 gels with surface-immobilized Fn.

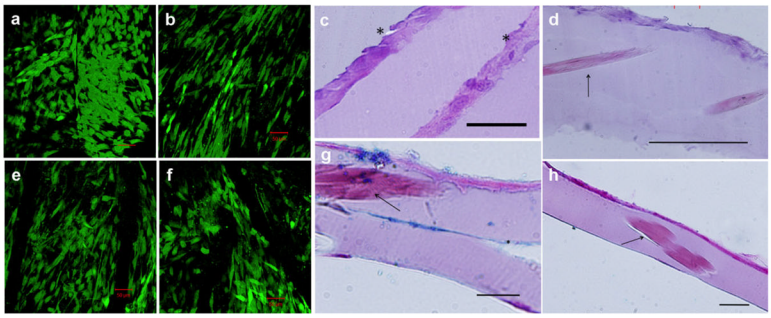

FIGURE 9.

Confocal microscopy and histology of multilayer protein sheets. Cell-seeded constructs were incubated in calcein AM solution for 1 h prior to confocal imaging in (a,b,e, and f). (a) Viable MSCs within a two-layer protein-sheet construct. (b,e,f) Cell viability within a tri-lamellar construct is visualized on the top, middle, and bottom layers, respectively. Histological analysis of MSC-seeded protein fiber sheets, stained with H&E and viewed in cross-section, is shown in (c,d,g, and h). (c) Tri-lamellar construct after 1 week in culture demonstrates limited MSC infiltration through the layers, with weak interlamellar bonding. Asterisks denote the layer interfaces. (d) A single protein sheet after 72 h in culture demonstrates MSC adhesion to the surface and embedded collagen fibers. (g) Alcian blue stain with nuclear fast red counterstain of a single sheet reveals limited glycosaminoglycan deposition and partial delamination. (h) Full-thickness image of a single sheet. Arrows indicate the presence of collagen fibers. Scale bars 50 μm.

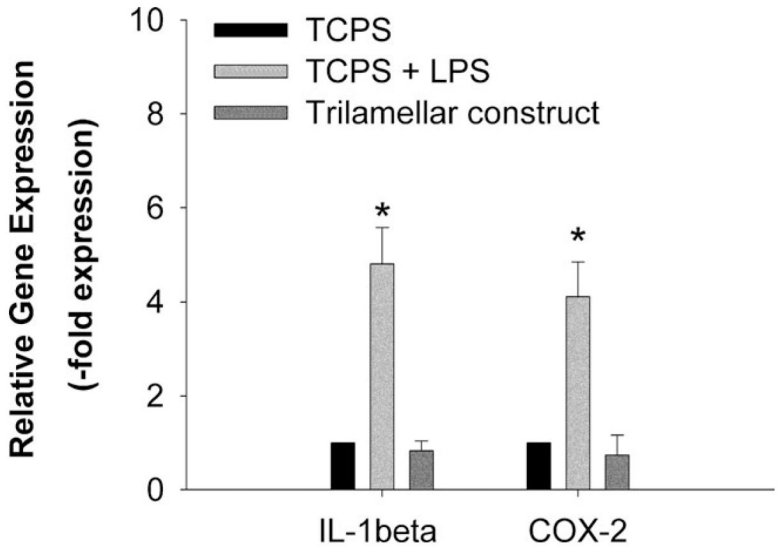

FIGURE 10.

Relative interleukin-1β and cyclooxygenase-2 gene expression by porcine MSCs. Cells were cultured on tissue culture polystyrene (TCPS, negative control), TCPS with 10 μg/mL LPS (positive control), and tri-lamellar protein sheets for 96 h. The housekeeping gene GAPDH was used as an endogenous control. Data were normalized to the TCPS negative control. * $p < 0.01$ compared to the TCPS negative control. For all groups, $n = 3$.